PROCEEDINGS OF SCIENCE

Freeze-out parameters: lattice QCD meets heavy-ion experiments

Sz. Borsányi[1], **Z. Fodor**[1,2,3], **S. D. Katz**[2,4], **S. Krieg**[1,3], **C. Ratti***[5], **K. K. Szabó**[1]

[1] *Department of Physics, Wuppertal University, Gaussstr. 20, D-42119 Wuppertal, Germany*
[2] *Inst. for Theoretical Physics, Eötvös University,*
Pázmány P. sétány 1/A, H-1117 Budapest, Hungary
[3] *Jülich Supercomputing Centre, Forschungszentrum Jülich, D-52425 Jülich, Germany*
[4] *MTA-ELTE "Lendület" Lattice Gauge Theory Research Group,*
Pázmány P. sétány 1/A, H-1117 Budapest, Hungary
[5] *Dip. di Fisica, Università di Torino and INFN, Sezione di Torino*
via Giuria 1, I-10125 Torino, Italy
E-mail: rattii@to.infn.it

We present continuum extrapolated lattice QCD results for higher-order fluctuations of conserved charges at finite-temperature. By comparing the numerical results obtained in the grand canonical ensemble on the lattice to the moments of net-charge and net-baryon distributions measured in heavy ion experiments, the temperature and the chemical potential may be estimated at the time of chemical freeze-out.

QCD-TNT-III-From quarks and gluons to hadronic matter: A bridge too far?,
2-6 September, 2013
European Centre for Theoretical Studies in Nuclear Physics and Related Areas (ECT), Villazzano, Trento (Italy)*

*Speaker.

PoS(QCD-TNT-III)033

1. Introduction

The QCD transition from a hadronic, confined system to a partonic one at zero baryo-chemical potential is an analytic cross-over, as was unambiguously shown by lattice QCD simulations [1]. This feature extends to small chemical potentials, covered by the high energy runs at RHIC. The possibility that the transition becomes first order at large chemical potentials has triggered the low energy runs at RHIC, soon to be followed by the CBM experiment at the GSI, in search for the elusive critical point. In order to successfully spot its position, one needs to define observables which are sensitive to the change in the order of the phase transition. Event-by-event higher order fluctuations of conserved charges are expected to diverge in the presence of a first order phase transition, and have therefore been proposed long ago to this purpose [2, 3, 4].

Parallel to the experimental effort lattice field theory has been able to describe the QCD transition with increasing precision. The transition temperature has been determined [5, 6], and the curvature of the transition line was also given [7]. The equation of state has been calculated at zero [8, 9] and small chemical potentials [10]. Quark number susceptibilities have also been determined both for strange as well as light flavors [11, 12]. All these observables have been extrapolated to the continuum limit.

The chemical freeze-out, defined as the last inelastic scattering of hadrons before detection, has already been characterized in terms of temperature and chemical potential, by fitting the pion, kaon, proton and other accessible particle yields from experiment within the statistical hadronization model [13, 14]. For higher collision energies, smaller chemical potentials are realized at freeze-out. Repeating the analysis for a series of beam energies yields several $(T-\mu)$ pairs on the phase diagram. The ever-increasing accuracy of fluctuation measurements at RHIC and LHC allows us today to make direct comparisons of lattice results with data. The STAR experiment has recently published the beam-energy and centrality dependence of the net-proton distribution [15]. For the net electric charge distribution there are preliminary results available both from the STAR [16, 17] and from the PHENIX collaborations [18].

The strategy for a successful comparison between theory and experiment has been defined in several steps [19, 20, 21]. Here we use the observables suggested in Ref. [22]. The fluctuations for a conserved quantum number, such as electric charge, are measured in a sub-system, small enough to behave like a grand canonical ensemble, yet large enough to behave like an ensemble. The selection of a subsystem is accomplished through cuts in rapidity and transverse momentum. Still, the fluctuations or even the mean value of net charge depends on the unknown subvolume. To cancel this factor, ratios of fluctuations are usually considered.

In this contribution, we show the continuum-extrapolated results for higher order fluctuations of electric charge and baryon number, which can be compared to the final, efficiency-corrected experimental data, once they become available [28].

2. Fluctuations from the lattice

Similarly to previous works, we choose a tree-level Symanzik improved gauge, and a stout-improved staggered fermionic action (see Ref. [23] for details). The stout-smearing [24] reduces taste violation (this kind of smearing has one of the smallest taste violations among the ones used

in the literature for large scale thermodynamic simulations, together with the HISQ action [25, 26] used by the hotQCD collaboration). This lattice artifact needs to be kept under control when studying higher order fluctuations of electric charge, which are pion-dominated at small temperatures, and thus particularly sensitive to this issue.

The continuum extrapolation is mainly performed on the basis of five lattice spacings, corresponding to temporal lattice extents of $N_t = 6,\ 8,\ 10,\ 12,\ 16$ (around T_c these extents result in lattice spacings of $a = 0.22, 0.16, 0.13, 0.11$ and 0.08 fm, respectively). At every lattice spacing and temperature we analyzed every 10th configuration in the rational hybrid Monte Carlo streams with 128...256 quartets of random sources. The statistics for each point is shown in Fig. 1. We follow the extrapolation strategy that we have discussed in Ref. [11], and perform several possible continuum fits (with and without a beyond-a^2 term, keeping or dropping the coarsest lattice, using tree-level improvement [8] or not, fitting the observable or the reciprocal of the observable, choosing between two possible interpolations). Weighting these continuum results by the goodness of the fit a histogram is formed, the width of which defines the systematic error (for details see Ref. [27]). In this paper we show the combined systematic and statistical errors on the continuum data.

In a grand canonical ensemble we obtain the fluctuations as derivatives of the partition function with respect to the chemical potentials:

$$\frac{\chi^{BSQ}_{lmn}}{T^{l+m+n}} = \frac{\partial^{\,l+m+n}(p/T^4)}{\partial(\mu_B/T)^l \partial(\mu_S/T)^m \partial(\mu_Q/T)^n}. \tag{2.1}$$

and they are related to the moments of the distributions of the corresponding conserved charges by

$$\begin{aligned} \text{mean}: \ M = \chi_1 \qquad & \text{variance}: \ \sigma^2 = \chi_2 \\ \text{skewness}: \ S = \chi_3/\chi_2^{3/2} \qquad & \text{kurtosis}: \ \kappa = \chi_4/\chi_2^2 \,. \end{aligned} \tag{2.2}$$

With these moments we can express the volume-independent ratios

$$\begin{aligned} S\sigma = \chi_3/\chi_2 \quad ; \quad & \kappa\sigma^2 = \chi_4/\chi_2 \\ M/\sigma^2 = \chi_1/\chi_2 \quad ; \quad & S\sigma^3/M = \chi_3/\chi_1 \,. \end{aligned} \tag{2.3}$$

The experimental conditions are such, that the three chemical potentials μ_B, μ_Q and μ_S are not independent of each other: the finite baryon density in the system is generated by the nucleon stopping in the collision region, and is therefore due to light quarks only. Strangeness conservation then implies that the strangeness density $\langle n_S \rangle = 0$. Similarly, the initial isospin asymmetry of the colliding nuclei yields a relationship between the electric charge and baryon-number densities: $\langle n_Q \rangle = Z/A \langle n_B \rangle$. For Au-Au and Pb-Pb collisions, a good approximation is to assume $Z/A = 0.4$.

Therefore, the dependence of μ_Q and μ_S on μ_B needs to be defined so that these conditions are satisfied. We take care of this by Taylor-expanding the densities with respect to the three chemical potentials up to order μ_B^3 [22]:

$$\begin{aligned} \mu_Q(T,\mu_B) &= q_1(T)\mu_B + q_3(T)\mu_B^3 + ... \\ \mu_S(T,\mu_B) &= s_1(T)\mu_B + s_3(T)\mu_B^3 + ... \end{aligned} \tag{2.4}$$

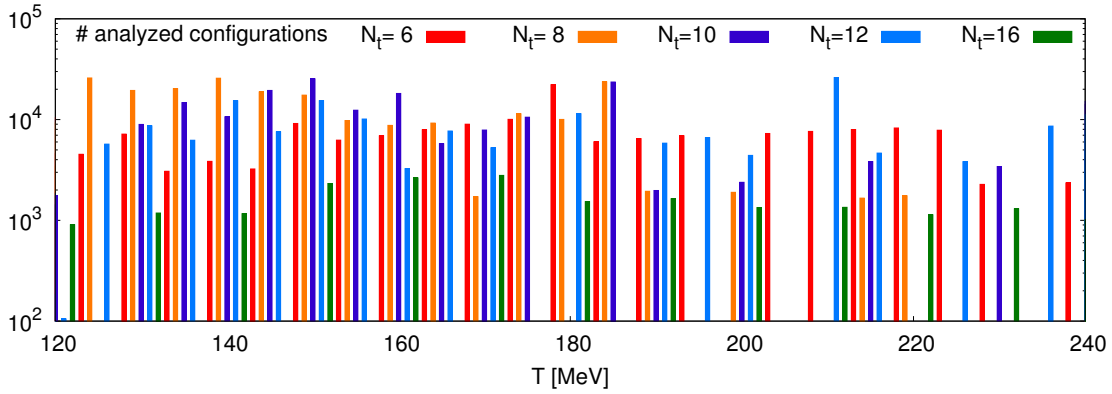

Figure 1: Statistics behind the fluctuation calculations. The stored configurations have been separated by 10 HMC trajectories, each. Each configuration was analyzed by $(128\ldots256)\times 4$ random sources.

These equations define q_1, q_3 and s_1 and s_3, respectively. Our continuum extrapolated data for the functions $q_1(T)$, $q_3(T)$, $s_1(T)$, $s_3(T)$ are shown in Fig. 2. Our data are compared to the BNL-Bielefeld group's result, where q_1 and s_1 was continuum extrapolated. They obtained q_3 and s_3 from $N_t = 8$ lattices using the HISQ action [22].

The chemical potential dependence enters through the fermion determinant ($\det M_i$), allowing for one μ_i parameter for each of the three dynamical flavor $i = u,d,s$. The actual observables are based on the derivatives of the logarithm of these determinants:

$$A_j \;= \frac{d}{d\mu_j}\log(\det M_j)^{1/4} = \;\frac{1}{4}\mathrm{Tr}M_j^{-1}M_j', \tag{2.5}$$

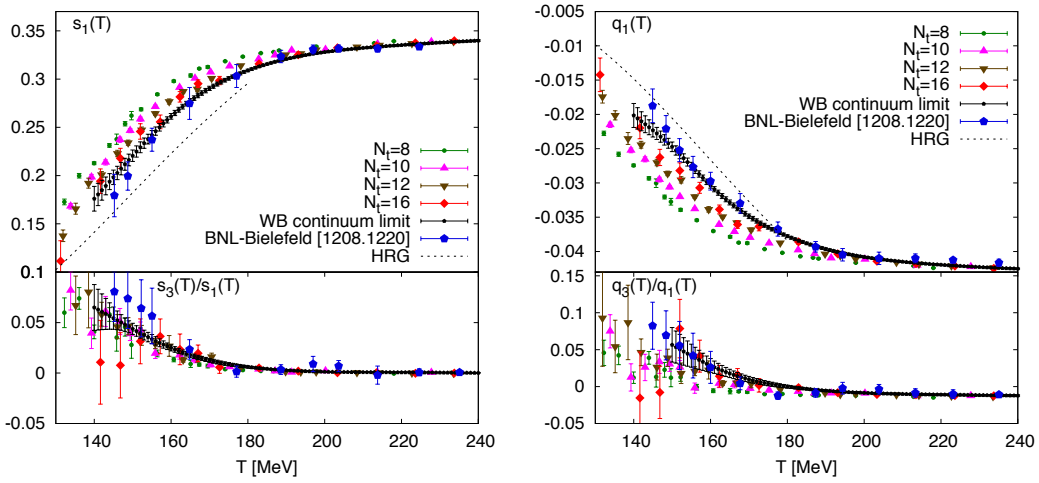

Figure 2: Upper panels: leading order contribution in μ_B for the strangeness (left figure) and the electric charge (right figure) chemical potentials. The lower panels show the corresponding NLO contributions. In all panels, the black dots correspond to the continuum extrapolated results. The BNL-Bielefeld results are shown as blue pentagons.

$$B_j = \tfrac{d^2}{(d\mu_j)^2}\log(\det M_j)^{1/4} = \frac{1}{4}\mathrm{Tr}\left(M_j'' M_j^{-1} - M_j' M_j^{-1} M_j' M_j^{-1}\right), \tag{2.6}$$

$$C_j = \tfrac{d^3}{(d\mu_j)^3}\log(\det M_j)^{1/4} = \frac{1}{4}\mathrm{Tr}\left(M_j' M_j^{-1} - 3M_j'' M_j^{-1} M_j' M_j^{-1} + 2M_j' M_j^{-1} M_j' M_j^{-1} M_j' M_j^{-1}\right), \tag{2.7}$$

$$D_j = \tfrac{d^4}{(d\mu_j)^4}\log(\det M_j)^{1/4} = \frac{1}{4}\mathrm{Tr}\left(M_j'' M_j^{-1} - 4M_j' M_j^{-1} M_j' M_j^{-1} + 12M_j'' M_j^{-1} M_j' M_j^{-1} M_j' M_j^{-1} - 3M_j'' M_j^{-1} M_j'' M_j^{-1} - 6M_j' M_j^{-1} M_j' M_j^{-1} M_j' M_j^{-1} M_j' M_j^{-1}\right). \tag{2.8}$$

We calculate these traces for every configuration using $(128\ldots256)\times 4$ random sources. The final derivatives emerge as connected and disconnected contributions, e.g. to second order we have

$$\partial_i \partial_j \log Z = \langle A_i A_j \rangle + \delta_{ij} \langle B_i \rangle . \tag{2.9}$$

Where products of diagrams appear, a disjoint set of random sources are used, like here in A_i and A_j, even when $i = j$. The first (disconnected) term is responsible for most of the noise, lattice artefacts, on the other hand, come mainly from the connected contributions.

3. Results

The quantities that we look at, in order to extract the freeze-out temperature and baryon chemical potential, are the ratios $R_{31}^Q(T,\mu_B) = \chi_3^Q/\chi_1^Q$ and $R_{12}^Q(T,\mu_B) = \chi_1^Q/\chi_2^Q$ for small chemical potentials, where $\mu_Q(\mu_B)$ and $\mu_S(\mu_B)$ are chosen to satisfy Eqs. (2.4). We also calculated the analogous baryon fluctuations (for details, see the journal version of this work [28]):

$$R_{31}^Q(T,\mu_B) = \frac{\chi_3^Q(T,\mu_B)}{\chi_1^Q(T,\mu_B)} = \frac{\chi_{31}^{QB}(T,0) + \chi_4^Q(T,0) q_1(T) + \chi_{31}^{QS}(T,0) s_1(T)}{\chi_{11}^{QB}(T,0) + \chi_2^Q(T,0) q_1(T) + \chi_{11}^{QS}(T,0) s_1(T)} + \mathscr{O}(\mu_B^2) \tag{3.1}$$

$$R_{12}^Q(T,\mu_B) = \frac{\chi_1^Q(T,\mu_B)}{\chi_2^Q(T,\mu_B)} = \frac{\chi_{11}^{QB}(T,0) + \chi_2^Q(T,0) q_1(T) + \chi_{11}^{QS}(T,0) s_1(T)}{\chi_2^Q(T,0)} \frac{\mu_B}{T} + \mathscr{O}(\mu_B^3).$$

The leading order in χ_3^Q/χ_1^Q is independent of μ_B, which allows us to use R_{31}^Q to extract the freeze-out temperature. Once T_f has been obtained with this method, the ratio R_{12}^Q can then be used to determine μ_B. Notice that in Eq. (3.1) we write the expansion of R_{12}^Q, but in the plots we will show our results up to NLO.

In Fig. 3 we show the ratios R_{31}^Q (left) and R_{31}^B (right) as functions of the temperature. The continuum extrapolations are shown as black dots. For the charge fluctuations we used five lattice spacings. Baryon fluctuations are plagued by greater noise, but are less sensitive to cut-off effects;

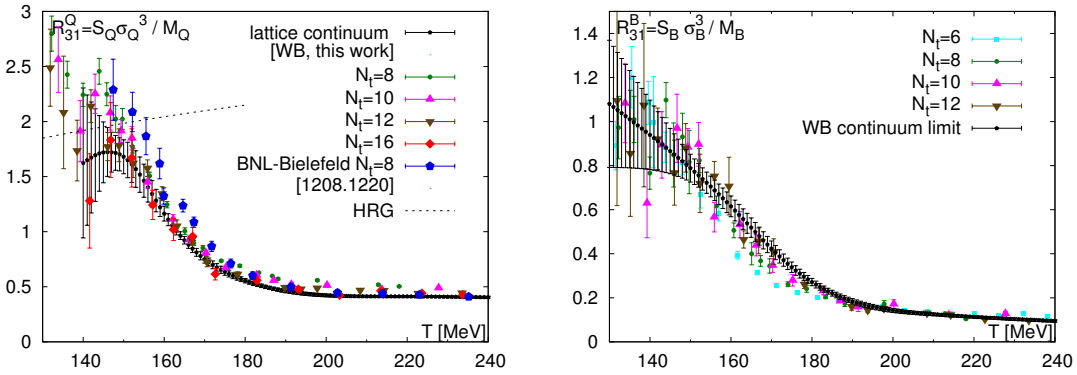

Figure 3: Lattice results on the skewness ratio for the charge (left) and the baryon number (right). The colored symbols correspond to lattice QCD simulations at finite-N_t. Black points correspond to the continuum extrapolation [28]; blue pentagons are the $N_t = 8$ results from the BNL-Bielefeld collaboration [22]

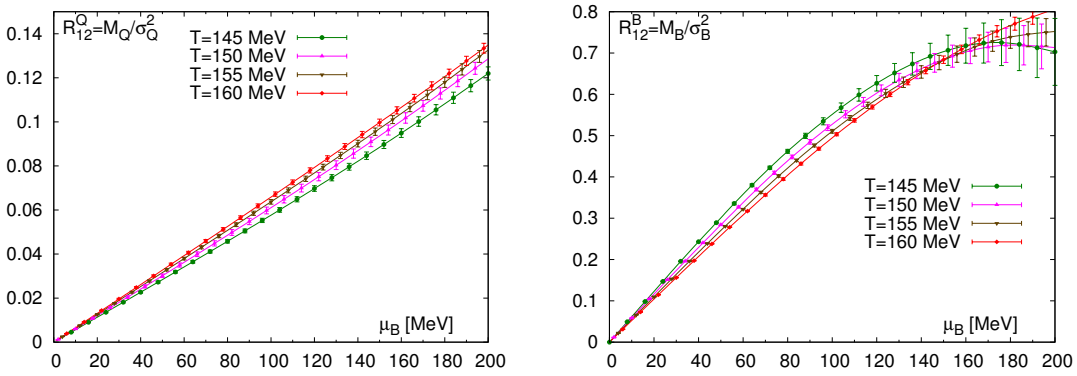

Figure 4: R^Q_{12} (left panel) and R^B_{12} as functions of μ_B: in both panels, the different colors correspond to the continuum extrapolated lattice QCD results, calculated in a range of temperatures around the QCD crossover [28].

here we used four spacings to obtain the continuum extrapolated results. Charge fluctuation results from the BNL-Bielefeld collaboration corresponding to $N_t = 8$ (from Ref. [22]) are also shown for comparison.

In Fig. 4 we show our results for R^Q_{12} and R^B_{12} as functions of the baryon chemical potential: the different curves correspond to different temperatures, in the range in which the freeze-out is expected. Such expectations may come from the arguments in Ref. [29] supporting a freeze-out just below the transition. Alternative hints come from the existing estimates from the statistical hadronization model [13, 14].

Notice that the ordering of the temperatures in Fig. 4 (left) and (right) is opposite. Thus, whether the chemical potentials from the charge and the baryon (proton) fluctuations deliver consistent results will very much depend on the associated temperature, which we can extract from the skewness analysis. A possible source for inconsistencies might be the comparison of proton fluctuation data with baryon fluctuations from the lattice, and also the remnant effects of baryon

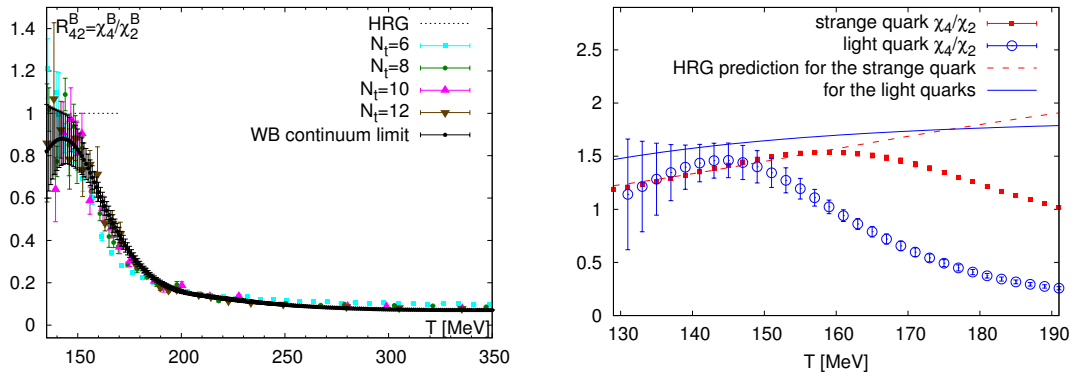

Figure 5: The baryon number (left) and flavor specific (right) kurtosis ($\kappa \times \sigma^2$) prediction from lattice QCD. These parameters are in principle accessible to LHC experiments, and may be used to define the freeze-out temperature for specific flavors, or for the system as a whole.

number conservation [30]. A cross-check between the freeze-out parameters from proton and electric charge data will also allow to test the basic assumption of thermal equilibrium at the time of freeze-out.

Finally, we show the kurtosis data in the continuum limit in Fig. 5. The kurtosis of baryon number and light vs. strange quark numbers show different sensitivity to temperature: the maxima and the deviation points from the hadron resonance gas prediction turn out to be flavor-dependent. The great question that the experiment will have to decide is whether the freeze-out temperatures themselves are flavor dependent [31].

Acknowledgments: This project was funded by the DFG grant SFB/TR55. The work of C. Ratti is supported by funds provided by the Italian Ministry of Education, Universities and Research under the Firb Research Grant RBFR0814TT. S. D. Katz is funded by the ERC grant ((FP7/2007-2013)/ERC No 208740) as well as the "Lendület" program of the Hungarian Academy of Sciences ((LP2012-44/2012). The numerical simulations were in part performed the GPU cluster at the Wuppertal University as well as on QPACE, funded by the DFG. We acknowledge PRACE for awarding us access to the Blue Gene/Q system (JUQUEEN) at Forschungszentrum Jülich, Germany.

References

[1] Y. Aoki, G. Endrodi, Z. Fodor, S. D. Katz and K. K. Szabo, Nature **443**, 675 (2006)

[2] M. A. Stephanov, K. Rajagopal and E. V. Shuryak, Phys. Rev. D **60**, 114028 (1999) [hep-ph/9903292].

[3] R. V. Gavai and S. Gupta, Phys. Rev. D **78**, 114503 (2008) [arXiv:0806.2233 [hep-lat]].

[4] M. Cheng, *et al.*, Phys. Rev. D **77**, 014511 (2008) [arXiv:0710.0354 [hep-lat]].

[5] Y. Aoki, *et al.* Phys. Lett. B **643** (2006) 46; Y. Aoki, *et al.* JHEP **0906** (2009) 088; S. Borsanyi *et al.* [Wuppertal-Budapest Coll.], JHEP **1009**, 073 (2010)

[6] A. Bazavov, T. Bhattacharya, M. Cheng, C. DeTar, H. T. Ding, S. Gottlieb, R. Gupta and P. Hegde *et al.*, Phys. Rev. D **85** (2012) 054503 [arXiv:1111.1710 [hep-lat]].

[7] G. Endrodi, Z. Fodor, S. D. Katz and K. K. Szabo, JHEP **1104** (2011) 001 [arXiv:1102.1356 [hep-lat]].

[8] S. Borsanyi, G. Endrodi, Z. Fodor, A. Jakovac, S. D. Katz, S. Krieg, C. Ratti and K. K. Szabo, JHEP **1011** (2010) 077 [arXiv:1007.2580 [hep-lat]].

[9] S. Borsanyi, Z. Fodor, C. Hoelbling, S. D. Katz, S. Krieg and K. K. Szabo, arXiv:1309.5258 [hep-lat].

[10] S. .Borsanyi, G. Endrodi, Z. Fodor, S. D. Katz, S. Krieg, C. Ratti and K. K. Szabo, JHEP **1208** (2012) 053 [arXiv:1204.6710 [hep-lat]].

[11] S. Borsanyi, Z. Fodor, S. D. Katz, S. Krieg, C. Ratti and K. Szabo, JHEP **1201** (2012) 138 [arXiv:1112.4416 [hep-lat]].

[12] A. Bazavov *et al.* [HotQCD Collaboration], Phys. Rev. D **86** (2012) 034509 [arXiv:1203.0784 [hep-lat]].

[13] A. Andronic, P. Braun-Munzinger and J. Stachel, Nucl. Phys. A **772** (2006) 167 [nucl-th/0511071] ; Phys. Lett. B **673** (2009) 142 [Erratum-ibid. B **678** (2009) 516] [arXiv:0812.1186 [nucl-th]].

[14] J. Cleymans, H. Oeschler, K. Redlich and S. Wheaton, Phys. Rev. C **73** (2006) 034905 [hep-ph/0511094].

[15] L. Adamczyk *et al.* [STAR Collaboration], arXiv:1309.5681 [nucl-ex].

[16] D. McDonald [STAR Coll.], arXiv:1210.7023 [nucl-ex].

[17] N. R. Sahoo [STAR Coll.], arXiv:1212.3892 [nucl-ex].

[18] J. T. Mitchell [PHENIX Collaboration], Nucl. Phys. A **904-905** (2013) 903c [arXiv:1211.6139 [nucl-ex]].

[19] S. Jeon and V. Koch, Phys. Rev. Lett. **85**, 2076 (2000)

[20] M. Asakawa, U. W. Heinz and B. Muller, Phys. Rev. Lett. **85**, 2072 (2000)

[21] F. Karsch, Central Eur. J. Phys. **10** (2012) 1234 [arXiv:1202.4173 [hep-lat]].

[22] A. Bazavov, H. T. Ding, P. Hegde, O. Kaczmarek, F. Karsch, E. Laermann, S. Mukherjee and P. Petreczky *et al.*, Phys. Rev. Lett. **109** (2012) 192302 [arXiv:1208.1220 [hep-lat]].

[23] Y. Aoki, *et al.* JHEP **0601**, 089 (2006)

[24] C. Morningstar and M. J. Peardon, Phys. Rev. D **69**, 054501 (2004)

[25] A. Bazavov and P. Petreczky, PoS **LAT2009**, 163 (2009)

[26] A. Bazavov and P. Petreczky, arXiv:1005.1131 [hep-lat].

[27] S. Durr, Z. Fodor, J. Frison, C. Hoelbling, R. Hoffmann, S. D. Katz, S. Krieg and T. Kurth *et al.*, Science **322** (2008) 1224 [arXiv:0906.3599 [hep-lat]].

[28] S. Borsanyi, Z. Fodor, S. D. Katz, S. Krieg, C. Ratti and K. K. Szabo, Phys. Rev. Lett. **111** (2013) 062005 [arXiv:1305.5161 [hep-lat]].

[29] P. Braun-Munzinger, J. Stachel and C. Wetterich, Phys. Lett. B **596** (2004) 61

[30] A. Bzdak, V. Koch and V. Skokov, Phys. Rev. C **87** (2013) 014901 [arXiv:1203.4529 [hep-ph]].

[31] R. Bellwied, S. Borsanyi, Z. Fodor, S. DKatz and C. Ratti, Phys. Rev. Lett. **111** (2013) 202302 [arXiv:1305.6297 [hep-lat]].